Check for updates

Received: 28 June 2024 | Revised: 19 August 2024 | Accepted: 11 September 2024

DOI: 10.1002/htj.23193

ORIGINAL ARTICLE

HEAT TRANSFER WILEY

Influence of anodization on the entropy generation in grooved heat pipes

A. Brusly Solomon[1] | **G. Jims John Wessley**[2] | **Madhu Ganesh**[2] | **Mohsen Sharifpur**[3,4] | **Renjith Singh Rethinam**[5]

[1]Micro and Nano Heat Transfer Lab, Centre for Research in Material Science and Thermal Management, Department of Mechanical Engineering, Karunya Institute of Technology and Sciences, Coimbatore, India

[2]Department of Aerospace Engineering, Karunya Institute of Technology and Sciences, Coimbatore, India

[3]School of Mechanical, Industrial and Aeronautical Engineering, University of the Witwatersrand, Johannesburg, South Africa

[4]Department of Medical Research, China Medical University Hospital, China Medical University, Taichung, Taiwan

[5]Department of Mechanical Engineering, Friedrich-Alexander-Universität Erlangen-Nürnberg, Erlangen, Germany

Correspondence

A. Brusly Solomon, Micro and Nano Heat Transfer Lab, Centre for Research in Material Science and Thermal Management, Department of Mechanical Engineering, Karunya Institute of Technology and Sciences, Coimbatore-641114, India.
Email: abruslysolomon@gmail.com

Mohsen Sharifpur, School of Mechanical, Industrial and Aeronautical Engineering, University of the Witwatersrand, Johannesburg, South Africa.
Email: mohsen.sharifpur@up.ac.za

Abstract

The present research deliberates the influence of anodization on the entropy reduction in heat pipes that have grooved wicks and are charged with anhydrous ammonia fluid. Entropy generation analysis indicates how much energy is squandered because of the poor heat transfer surface, and the entropy must be minimized at any cost for a better environment. Anodization was performed to form a thin porous layer with micro/nanostructured pores in the grooved heat pipe's (GHP's) interior surface. The test findings demonstrate that the anodized thin porous layer enhances capillary rise and accelerates heat transmission. The entropy generation was computed by utilizing the heat transfer between the evaporator and condenser of a GHP and the drop in pressure across it. The second-law efficiency and overall entropy generation are also examined in this study. The findings demonstrate that for a GHP with a groove size of 400 μm (0.4 mm) and a thin porous covering, the lowest entropy generation owing to heat transfer across a heat pipe is 0.015 W/K and the overall entropy generation is 0.02 W/K. Also, the same anodized GHP receives a maximum second-law efficiency of 89.12%. This investigation revealed that the thin porous coating through anodization is the prime reason for the entropy reduction in the heat pipe.

 © 2024 Wiley Periodicals LLC.

Funding information
Department of Science and Technology, Government of India; DST–SERB, Grant/Award Number: DST/SERB/YSS/2015/001084

KEYWORDS
anodization, anodized grooves, entropy generation, second-law efficiency, thin porous coating

1 | INTRODUCTION

The concept of entropy minimization has been applied extensively in recent years, particularly in thermal and electronic devices, because the standard design methodologies do not guarantee thermodynamic design efficiency. Therefore, the entropy generation in heat transfer devices should decrease to improve performance. The estimation of second-law efficiency is a vital parameter for estimating the entropy generation in heat transfer devices. Reducing the entropy generation through the design of a proficient heat transfer (cooling) device will undoubtedly improve the second-law efficiency, potentially allowing it to be used in electronic cooling applications. By looking into the concept of electronic cooling, the constant addition of new features and component downsizing in electronic devices leads to increased heat generation in the processors. However, electronic equipment manufacturers forecast that the component failure rate doubles for every 10° increase in temperature.[1]

Further, the type of cooling approaches, such as single-phase and multiphase cooling, is considered the dependent factor for the cause of entropy generation. On comparing single-phase cooling, two-phase cooling processes involving evaporation and condensation proved to be the vital cooling method for minimizing the generation of entropy.[2] A heat pipe is considered an efficient heat-exchanging device that operates on the evaporation and condensation principle and can exchange heat from one end to another with the help of coolant movement. A coolant is a phase-change medium that absorbs and releases latent heat during the evaporation and condensation processes. Furthermore, the thermophysical attributes of conventional fluids[3–5] and nanofluids,[6–8] various types of wicks such as *Microsorum fortunei* structural-like wick,[9] and modifications such as the construction of grooves,[10] microembossing molds,[11] chemically treated surface, and anodized surface[12–15] are notorious for impacting the performance of both heat pipes and thermosyphons. Later, it was realized that the surface alterations in the heat-absorbing surface have a predominant role in heat transfer due to additional capillary performance and surface wettability. Furthermore, in heat pipes, it was proved that the entropy generation could be reduced (1) when the existence of a thermodynamic condition, that is, the vapor temperature, is higher than the external heating and cooling state to achieve effective functioning, (2) there is an optimum ambient condenser temperature, (3) by the removal of insulation from the adiabatic section, and (4) by considering smaller evaporator along with higher wick area to achieve the practical function of heat pipe.[16]

Several studies have been performed to analyze the rate of entropy generation by primarily considering the influence of working fluid and the architecture of the devices. Nanofluids' application minimizes entropy generation and enhances heat transfer performance due to increased thermal conductivity compared to conventional liquids such as water, acetone, and oils. Ghanbarpour and Khodabandeh[2] observed that the entropy generation decreased when a tubular heat pipe was operated with Al_2O_3 and TiO_2/DI water-based nanofluids. Kim et al.[17] analyzed the irreversibility of the U-bend pulsating heat pipe numerically, considering the effect of pressure losses and wall temperatures. It was concluded that the wall temperatures, the mass of vapor, and the frequency of oscillations were the reason for entropy generation in

26884542, 2025, 1, Downloaded from https://onlinelibrary.wiley.com/doi/10.1002/htj.23193 by University Of Pretoria, Wiley Online Library on [06/08/2025]. See the Terms and Conditions (https://onlinelibrary.wiley.com/terms-and-conditions) on Wiley Online Library for rules of use; OA articles are governed by the applicable Creative Commons License

the U-bend pulsating heat pipe. Akbarzadeh et al.[18] examined a double-pipe heat-exchanging device's thermal performance and entropy generation with porous inserts. The inserts were introduced at four locations inside the heat exchanger: the wall surface, the central core, and the inner and outer wall surface. Entropy generation and heat transport analysis and the impact of porous media's thermal conductivity and Darcy number were studied. The results showed that the porous material inserted in the heat exchanger's central component experiences the highest entropy generation. Also, the generation of entropy due to the viscous effect was higher on the inner wall surface than on the outer wall. Jafarmadar et al.[19] numerically analyzed the thermal performance and entropy of pulsating heat pipes filled with aluminum oxide, silver, and CuO nanofluids as coolants. This investigation examines how particle size, shape, and volume concentration affect heat transfer efficiency. The study concludes that the nanofluids in heat pipes enhance thermal conductivity, thereby increasing performance and reducing entropy generation. Comparing three working fluids, Al_2O_3 and CuO nanofluids show similar performance and more reduction in entropy generation. Silver nanofluids show a decrease in thermal enactment and higher generation in entropy due to the deferred oscillation and generation of bubbles. Furthermore, entropy due to frictional drop in pressure has nil impact on the total entropy. Kumar et al.[20] mathematically analyzed the microchannel's heat transfer performance and entropy generation using graphene + silver nanofluid as a working medium. The nanoparticle quantity and inlet velocity of fluid effect on thermal enactment and generation of entropy were analyzed. In summary, it was found that increasing the nanoparticle quantity and velocity of the fluid reduces evaporator temperature and resistance. The entropy study revealed that the higher nanofluid volume concentration results in higher frictional entropy, lower Bejan number, and total entropy generation. Further, this study recommends using nanofluids as a microchannel coolant to increase thermal performance and reduce entropy generation. Chopra et al.[21] estimated the heat pipe's thermodynamic and techno-economic efficiency with an evacuated tube collector charged with deionized (DI) water as a coolant. This study focuses on energy, exergy analysis, and cost-effective parameters suitable for weather conditions. A heat pipe with an evacuated tube collector of 1.69 m^2 was fabricated and experimentally tested for different volume flow rates in the range of 20–60 LPH. From the test results, maximum energy and exergy efficiency of 72% and 5.2% were found at the volume flow rate of 60 LPH, whereas minimum energy and exergy efficiency of 55% and 1.3% were found at 20 LPH. Also, it was found that the heating system with an evacuated tube collector and heat pipe is more efficient in terms of both performance and reduced entropy generation than the direct heating system with only an evacuated tube collector. Khosravi-Bizhaem et al.[22] experimentally evaluated the heat transfer enactment, generation of entropy, and exergy destruction in helical tubes charged with silver, multiwalled carbon nanotubes (MWCNTs), and graphene oxide nanofluids as a coolant. This study also focuses on heat transfer, pressure losses, and entropy generation under $Re < 2300$ condition by providing constant heat flux. It was shown that the silver and MWCNTs in helical tubes enhance the heat transfer rate by 25% and 10%. In entropy studies, the usage of silver and MWCNTs in helical tubes was found to reduce the total entropy generation and exergy destruction. In contrast, graphene nanofluids decrease the performance and increase entropy generation due to the lower thermal conductivity of graphene nanoparticles. On comparing entropy results with the base fluid (DI water), silver/water nanofluids show a 15% reduction in entropy generation. Maqbool and Sadiq[23] formulated a mathematical model to study the thermal performance and entropy analysis using hyperbolic nanofluids as working fluid in a ciliated tube for medical application. This ciliated tube was used in the medical field where the development of embryos grows. The incorporation

26884542, 2025, 1, Downloaded from https://onlinelibrary.wiley.com/doi/10.1002/htj.23193 by University Of Pretoria, Wiley Online Library on [06/08/2025]. See the Terms and Conditions (https://onlinelibrary.wiley.com/terms-and-conditions) on Wiley Online Library for rules of use; OA articles are governed by the applicable Creative Commons License

of hyperbolic nanofluids in the ciliated tube reduces the growth of cysts, thereby destroying the development of embryos. The nonlinear equation in the mathematical model was developed using the Homotopy Perturbation Method and MATHEMATICA software. This study found that adding nanoparticles increases axial velocity and thermal conductivity. Further, entropy studies show that adding nanofluids decreases the entropy generation since there is a pressure drop. Ersöz and Yildiz[24] investigate the comparative thermoeconomic analysis of a two-phase closed thermosyphon charged with DI water, petroleum ether, and methanol as coolants. Experimentation was carried out for velocities ranging from 3.3 to 6.3 m/s. The test results show that the thermosyphon with methanol and petroleum ether reduced the exergy by about 56% and 12% over the use of DI water. Also, applying DI water in thermosyphon reduces the entropy generation and exergy over the other two working fluids. Hari and Muraleedharan.[25] analyzed the influence of irreversibility in flat heat pipes and their thermal characteristics. The nonlinear program was formulated using LINGO 15 software and the influence of entropy generation of flat heat pipe. It was illustrated that the generation of entropy could be reduced by raising the sink temperature, decreasing the adiabatic length, reducing the wick thickness, and increasing the mesh number. Behrooz and Ziapour[26] studied the influence of various refrigerants on the exergy of thermosyphon. The individual exergy analysis was carried out for different refrigerants. The results show that the water and R22 refrigerant show minimum and maximum mass flow rates during experimentation. Additionally, it was inferred that the higher heat transfer coefficient at the ambient section leads to reduced condenser exergy and total exergy.

The above studies show that entropy generation was minimized in various heat pipes, thermosyphons, and minichannels. The parameters such as working fluid, geometry, surface modification (coating), and heat input contributed more to the reduction in entropy generation and exergy, leading to performance enhancement. Similarly, parameters such as mesh number, wick thickness, and heat sink temperatures are altered to reduce the entropy generation in thermosyphons and heat pipes. Though many techniques and methods are applied to reduce entropy, the aforementioned methods were found costly. Hence, the objective of this study is to adopt a cost-effective method to reduce entropy generation and enhance the performance of heat pipes. The novelty of the work is the reduction of entropy generation using an anodized surface with semispherical pore formation in the interior surface of grooved heat pipes (GHPs), which is a simple and economical process. Further, a decrease in wall temperature was significant in anodized (surface-modified) heat pipes due to higher capillary rise, which could lead to more entropy reduction. Though the performance details of anodized heat pipes and thermosyphons are available in the open literature, no studies are available on the entropy generation of anodized devices. Thus, by considering the importance of reducing entropy generation in anodized heat pipes, this research focuses on studying the impact of anodization on the entropy generation of GHPs with different groove sizes using ammonia as a coolant.

2 | DETAILS OF EXPERIMENTATION

2.1 | Manufacturing of aluminum heat pipes with grooved wick

The aluminum tube with an outside diameter (OD), internal diameter, and total length of 19, 12.5, and 350 mm is considered for heat pipe fabrication. The total length of GHP (350 mm) was

26884542, 2025, 1, Downloaded from https://onlinelibrary.wiley.com/doi/10.1002/htj.23193 by University Of Pretoria, Wiley Online Library on [06/08/2025]. See the Terms and Conditions (https://onlinelibrary.wiley.com/terms-and-conditions) on Wiley Online Library for rules of use; OA articles are governed by the applicable Creative Commons License

divided into the evaporator (100 mm), adiabatic (100 mm), and condenser sections (150 mm), respectively. Primarily, the rectangular microgroove structure for the two sets of GHP was made using the electrical discharge machining process. The first set of GHP with a groove width of 500 μm (0.5 mm) and a depth of 2000 μm (2 mm) and the second set of GHP with a groove width of 400 μm (0.4 mm) and a depth of 2 mm were fabricated. The above two sets of GHPs were tested with nonanodized and anodized inner surfaces. The anodization (electrochemical process) was performed to form a thin micro/nanoporous coating on the interior surface of the two sets of GHP. The cathode and anode electrodes' voltage and current supplies are carefully controlled to achieve the semispherical pores during the anodization process. Initially, a voltage of 1 V is set during anodization, and related current data are tracked. After that, the voltage is raised by 1 V every minute to 15 V, and it stays at this level for 45 min. The pore development could be disrupted by a spike in the current of more than 5 A during this period. The current value was maintained below 5 A to guarantee the creation of semispherical pores. The anodized layer dissolves, and the pore widens and deepens when the current supply is allowed to exceed 5 A. Following this method, a cleaning process was done before the fabrication of GHP. Then, both ends of the GHP are closed with end caps. Next, an aluminum tube with an OD of 9.5 mm is fused to the condenser end for charging the working fluid. The necessary cleaning and evacuation process is done, and the required amount of ammonia is filled into the GHP for experimentation. Finally, the heating coil of nichrome material with two layers is winded to the evaporator for a heat supply before the testing.

2.2 | Investigational methods

Figure 1 shows the schematic illustration of the testing arrangement used for the study. The experimental setup comprises a chilling unit (temperature range of 0–50°C), heat supply unit (ranging between 0 and 500 W), flowmeter (ranging between 0 and 50 LPH), wattmeter, and

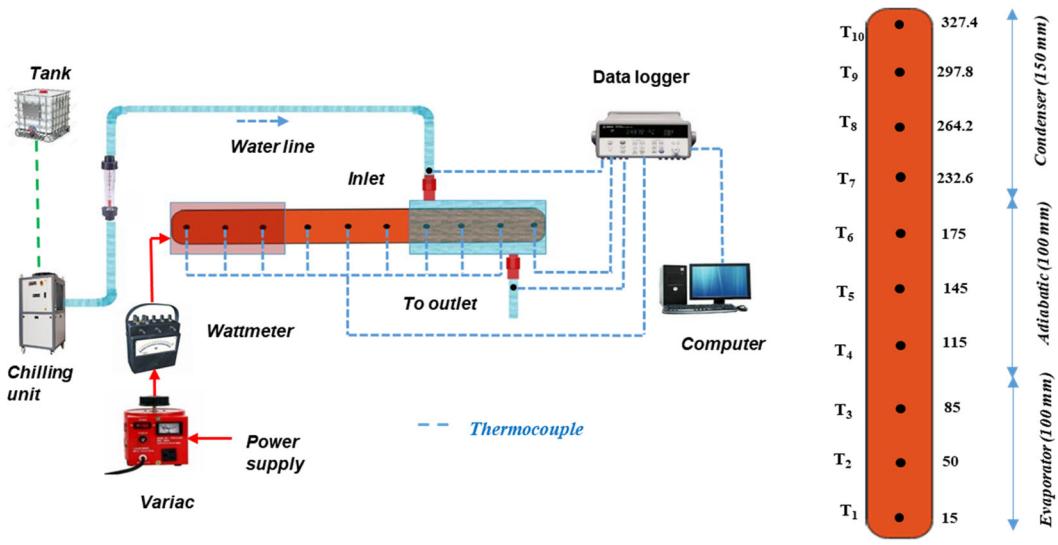

FIGURE 1 Schematic view of an experimental setup.

26884542, 2025, 1, Downloaded from https://onlinelibrary.wiley.com/doi/10.1002/htj.23193 by University Of Pretoria, Wiley Online Library on [06/08/2025]. See the Terms and Conditions (https://onlinelibrary.wiley.com/terms-and-conditions) on Wiley Online Library for rules of use; OA articles are governed by the applicable Creative Commons License

data logger system (with 22 channels). The GHP's condenser section is continuously flooded with cooling water at a constant rate of 20 LPH with a temperature of 10°C. In total, 12 thermocouples with ±0.2% accuracy are fixed on the total length of the heat pipe (four in the condenser, one in each of the inlet and outflow, three in the evaporator and adiabatic, and four in total), and then it is linked to data acquisition system where the data will be recorded and displayed in the computer. After all the instrumentation, heat input is given via Dimmerstat. The voltage and corresponding current values were taken from the respective indicators, and the heat input was calculated by multiplying the voltage and current applied to the heating coil. The heat input was applied with an interval of 5 W till it reached the steady state. In this experiment, the temperature of evaporator (T_e) is determined by averaging T_1, T_2, and T_3, the adiabatic temperature (T_a) is determined by averaging T_4, T_5, and T_6, and the condenser temperature (T_c) is determined by averaging T_7, T_8, T_9, and T_{10}. T_{11} and T_{12} are taken as water inlet and water outlet temperatures. The performance testing was done at the optimum confluence angle of 45°, and the data were recorded.[15] The accuracy of the flow meter and thermocouple used in the study are found to be ±3% and ±0.5%, respectively. The uncertainty estimated for the heat supplied is 1.5%, and the same for the entropy generation is less than 5%.

3 | DATA REDUCTION

The entropy generation is said to be zero, where all the reversible processes are quasistatic, which is considered the supreme objective. Also, the existence of friction or sliding forces indicates that the quasistatic process is not reversible. The present study is conducted at certain inclination angles; hence, the process is irreversible due to sliding or frictional forces, which leads to entropy generation in both nonanodized and anodized heat pipes. Moreover, in this nonanodized and anodized GHP, two main irreversibilities, heat transfer and irreversibility due to drop in pressure (liquid and vapor), may influence the entropy generation. Additionally, irreversibility destroys exergy and affects the second law of efficiency. Therefore, this study focuses on entropy generation along with the thermodynamic second-law approach of anodized and nonanodized GHP with variation in groove size using ammonia as a coolant.

3.1 | Entropy generation due to heat exchange between the evaporator and condenser

Entropy is generated when heat is exchanged between the evaporator and condenser in a thermodynamic cycle with little temperature change. Therefore, the second law of the thermodynamics approach is used to evaluate the entropy due to heat transfer, as presented in Equation (1).[2]

$$S_{HT} = \frac{Q}{T_c} - \frac{Q}{T_e}, \tag{1}$$

where Q is the input power applied, and T_e and T_c are the average evaporator and condenser temperatures (K), respectively.

26884542, 2025, 1, Downloaded from https://onlinelibrary.wiley.com/doi/10.1002/htj.23193 by University Of Pretoria, Wiley Online Library on [06/08/2025]. See the Terms and Conditions (https://onlinelibrary.wiley.com/terms-and-conditions) on Wiley Online Library for rules of use; OA articles are governed by the applicable Creative Commons License

3.2 | Entropy generation due to vapor flow

Entropy generation due to friction was caused by the movement of working fluid at vapor and liquid phases, respectively. Thus, the entropy due to friction is estimated using Equation (2):[2]

$$S_{\text{vapor}} = \frac{\dot{m} \cdot \Delta p_{\text{v}}}{\rho_{\text{v}} \cdot T_{\text{v}}}, \tag{2}$$

where $\dot{m}$ is the vapor mass flow rate, and Δp_{v}, ρ_{v}, and T_{v} are the vapor pressure, vapor density, and vapor temperature, respectively. Also, the mass flow rate can be estimated using Equation (3):

$$\dot{m} = \frac{\dot{Q}}{h_{\text{fg}}}, \tag{3}$$

where $\dot{Q}$ is the input power and h_{fg} is the latent heat of vaporization. Then, Δp_{v} will be calculated using Equation (5)[2]:

$$\Delta p_{\text{v}} = \frac{8\mu_{\text{v}} \times V \times L_{\text{eff}}}{R_{\text{v}}^2}, \tag{4}$$

where μ_{v}, V, L_{eff}, and R_{v} are the dynamic viscosity, vapor velocity, effective length of the heat pipe, and vapor channel radius, respectively. The effective length of a heat pipe is estimated as in Equation (5)[2]:

$$L_{\text{eff}} = \left\{\frac{l_{\text{e}} + l_{\text{c}}}{2}\right\} + l_{\text{a}}, \tag{5}$$

where l_{e}, l_{a}, and l_{c} are the length of the heat pipe's evaporator, adiabatic, and condenser sections, respectively.

3.3 | Entropy generation due to liquid flow in the wick

Similar to the entropy generation due to vapor flow, the same due to liquid flow inside the heat pipe is evaluated using Equation (6)[2]:

$$S_{\text{liquid}} = \frac{m \times \Delta p_{\text{l}}}{\rho_{\text{l}} \times T_{\text{c}}} \tag{6}$$

where the mass flow rate of the working fluid is denoted as m, and Δp_{l}, ρ_{l}, and T_{l} are a heat pipe's liquid in the condenser's pressure drop, density, and condenser liquid temperatures, respectively.

Then, liquid drop in pressure is estimated using Equation (7)[2]:

$$\Delta P_{\text{l}} = \frac{\mu_{\text{l}} \times L_{\text{eff}} \times Q}{\rho_{\text{l}} \times h_{\text{fg}} \times A_{\text{a}} \times K}, \tag{7}$$

26884542, 2025, 1, Downloaded from https://onlinelibrary.wiley.com/doi/10.1002/htj.23193 by University Of Pretoria, Wiley Online Library on [06/08/2025]. See the Terms and Conditions (https://onlinelibrary.wiley.com/terms-and-conditions) on Wiley Online Library for rules of use; OA articles are governed by the applicable Creative Commons License

where μ_l, L_{eff}, ρ_l, Q, h_{fg}, A_a, and K are the dynamic viscosity of a liquid, effective length, liquid density, heat load, latent heat of vaporization of liquid, anodized surface area, and permeability of the groove (including with and without anodization), respectively.

Permeability of the wick surface (K) is assessed using Equation (8)[2]:

$$K = \frac{2\varepsilon r_{hl}^2}{f_l Re_l}. \tag{8}$$

In Equation (8), the grooved wick's porosity is denoted as ε for both nonanodized and anodized surfaces, the hydraulic radius of the wick is given as r_{hl}, and the coefficient of drag is given as $f_l Re_l$. The r_{hl} of the wick is calculated as

$$r_{hl} = \frac{2LW}{2L + W}. \tag{9}$$

In Equation (9), the width and depth of grooves are represented as W and L, respectively. The drag coefficient in the wick due to condensate flow is calculated by

$$f_l Re_l = 24(1 - 1.355\alpha^* + 1.9467\alpha^{*2} - 1.7012\alpha^{*3} + 0.9564\alpha^{*4} - 0.2537\alpha^{*5}) \tag{10}$$

and

$$\alpha^* = \frac{W}{L}. \tag{11}$$

The parameters related to the anodized surface are taken from the scanning electron microscopy analysis conducted in our previous study[15] presented in Figure 2A–C.

Subsequently, the total entropy generated in the heat pipe for the two sets of GHPs due to the difference between the evaporator temperature and condenser temperature, liquid flow, and vapor flow is calculated using Equation (12)[2]:

$$S_{Total} = S_{HT} + S_{liquid} + S_{vapor}. \tag{12}$$

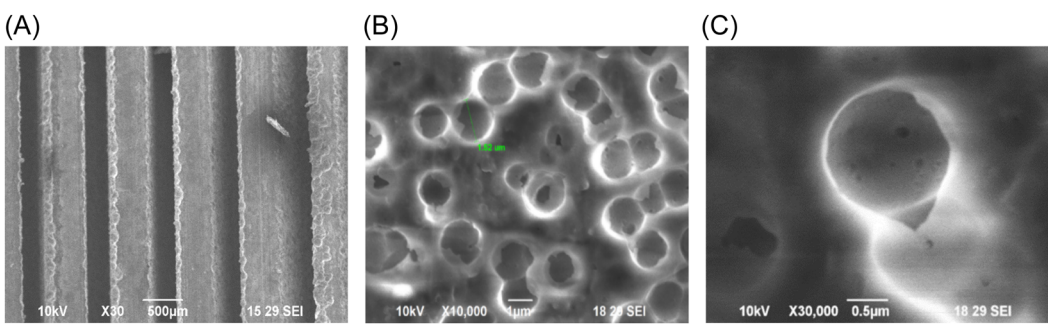

FIGURE 2 Scanning electron microscopy images of grooved anodized surfaces at a magnification of (A) 30x, (B) 10,000x, and (C) ×30,000.[15]

26884542, 2025, 1, Downloaded from https://onlinelibrary.wiley.com/doi/10.1002/htj.23193 by University Of Pretoria, Wiley Online Library on [06/08/2025]. See the Terms and Conditions (https://onlinelibrary.wiley.com/terms-and-conditions) on Wiley Online Library for rules of use; OA articles are governed by the applicable Creative Commons License

To identify whether the GHP is governed by irreversibility due to wall temperature or frictional fluid flow,[22]

$$Be = \frac{S_{\text{genHT}}}{S_{\text{genHT}} + S_{\text{genFF}}}, \tag{13}$$

where Be, S_{genHT}, and S_{genFF} indicate the Bejan number and generation in entropy due to thermal response and fluid flow, respectively.

3.4 | Second-law performance

As a known fact, the performance of any heat transfer device could be estimated by the second-law efficiency. It is the percentage of useful energy available to the heat transfer system compared to the utilized useful energy. Therefore, the second-law efficacy could be applied to evaluate the efficiency of both nonanodized and anodized GHP having two groove widths at an optimum inclination angle of 45°, as given in.[16]

$$\eta_{\text{II}=}\eta_{\text{I}}\left\{1 - \frac{1}{\left[\frac{T_{\text{e,v}}}{T_{\text{e,v}} - T_{\text{c,v}}} - 1\right]\left[\frac{T_{\text{e,v}}}{T_{\text{c,a}}} - 1\right]}\right\}, \tag{14}$$

where η_{I} is known as the first law efficiency of GHP, and $T_{\text{e,v}}$ and $T_{\text{c,v}}$ are the mean evaporator and condenser temperatures, respectively. $T_{\text{c,a}}$ is the ambient temperature at the condenser section, which is taken as 22°C.

4 | RESULTS AND DISCUSSIONS

In this study, the wall temperatures of different heat pipe sections, thermal resistance, and heat transfer coefficients were taken from our previous study[15] to estimate the entropy generation.

4.1 | Effect of anodization on the entropy generation due to heat transfer of GHP

The change in entropy generation linked to heat exchange between the evaporator and the condenser of both nonanodized and anodized GHPs at an optimal tilt angle of 45° is estimated using Equation (1), and the results are shown in Figure 3. It is found that the entropy increases linearly with rising heat input since the entropy and heat transfer are directly proportional to each other as per Equation (1). It is also found that the entropy of anodized GHP is lower than that of the nonanodized GHP. Further, the entropy of anodized GHP with a 0.4-mm groove size is lower than that of the same GHP with a 0.5-mm groove size. Since entropy is an estimation of irreversibility, it is found that the rise in heat load leads to an

26884542, 2025, 1, Downloaded from https://onlinelibrary.wiley.com/doi/10.1002/htj.23193 by University Of Pretoria, Wiley Online Library on [06/08/2025]. See the Terms and Conditions (https://onlinelibrary.wiley.com/terms-and-conditions) on Wiley Online Library for rules of use; OA articles are governed by the applicable Creative Commons License

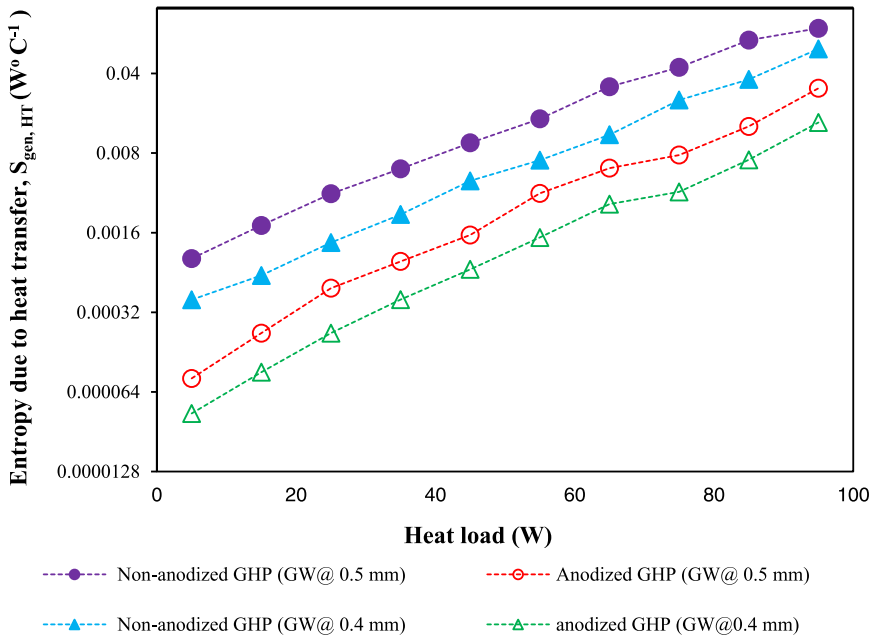

FIGURE 3 Impact of anodization on the heat transfer irreversibility of GHP. GHP, grooved heat pipe; GW, groove width.

increase in energy loss, as illustrated in Figure 3. Further, from Figure 3, a maximum entropy value of 0.099 W/°C and a minimum entropy value of 0.015 W/°C were found for non-anodized GHP having a GW of 0.5 mm and anodized GHP having a GW of 0.4 mm, respectively, at a heat input of 95 W. Furthermore, the decreased wall temperatures of the evaporation and condensation section lead to minimum entropy generation.

When heat is applied to the evaporator, it is conducted to the working fluid via the grooved structures. The presence of a groove structure improves the surface area and capillarity. The groove absorbs the heat and transfers it to the working fluid, vaporizing it. During this process, the liquid absorbs the latent heat and becomes vapor. Then the vapor reaches the condenser section, losing its latent heat and becoming liquid. As the cooling water circulates around the condenser section, the condensed fluid travels back rapidly to the evaporator through the groove surface, reducing entropy generation.

Furthermore, anodizing the inner layer of grooves forms the thin porous layer, thereby increasing the additional heat transfer surface area and capillarity.[15] Moreover, the thin porous coating and the formation of structured pores in the coating reduce the contact angle of the surface and enhance the capillary pressure as per the Young–Laplace equation. The Young–Laplace equation shows that capillary pressure $\Delta p = 2\sigma \operatorname{Cos} \theta / r_c$, in which θ is the contact angle, and the same decreases significantly from 110° to <10°[27] in the anodized surface and increases the capillary pressure. Thus, the formation of microstructure due to anodization helps to quick return of condensate from the GHP condenser to the evaporator through the anodized groove surface, resulting in decreased wall temperature and entropy generation. As an outcome, an anodized layer along with low GW (0.4 mm) GHP reduced almost 76.7% entropy generation compared to nonanodized GHP of the same GW.

26884542, 2025, 1, Downloaded from https://onlinelibrary.wiley.com/doi/10.1002/htj.23193 by University Of Pretoria, Wiley Online Library on [06/08/2025]. See the Terms and Conditions (https://onlinelibrary.wiley.com/terms-and-conditions) on Wiley Online Library for rules of use; OA articles are governed by the applicable Creative Commons License

4.2 | Effect of anodization on the generation of entropy due to vapor and liquid pressure drop of GHP

The drop in pressure is one of the critical elements to consider for evaluating the operational feasibility of a GHP since entropy is produced due to the irreversibility associated with friction. Figures 4 and 5 present the deviation in entropy generation due to the drop in vapor and liquid flow pressure, calculated using Equations (2) and (6) for the two sets of GHP at an optimum tilt angle of 45°. First, the drop in pressure arises in the GHPs mainly due to the frictional effect at their corresponding liquid and vapor lines. Figures 5 and 6 showed a linear increase in entropy generation due to a drop in the pressure of vapor and fluid with an increase in heat load. It was also found that the entropy due to the liquid and vapor flow of anodized GHP is lower than that of nonanodized GHP. Further, the entropy due to liquid and vapor flow of anodized GHP with a 0.4-mm groove size is lower than that of the same GHP with a 0.5-mm groove size. Further, it was noticed that the entropy generation due to the liquid and vapor flow (Figures 4 and 5) is lower than the entropy due to heat transfer (Figure 3). The reduced entropy generation due to vapor and liquid pressure drop is mainly due to low viscous flow, wall temperatures, and their concerned thermophysical properties of both sets of GHP. Further, anodization forms a thin micro/nanoporous coating that augments the heat transfer through evaporation, resulting in decreased entropy generation. On comparing all the cases, a minimum entropy of 1.21×10^{-3} W/°C due to vapor flow and 0.00354×10^{-3} W/°C due to liquid flow was found in anodized GHP having a GW of 0.4 mm.

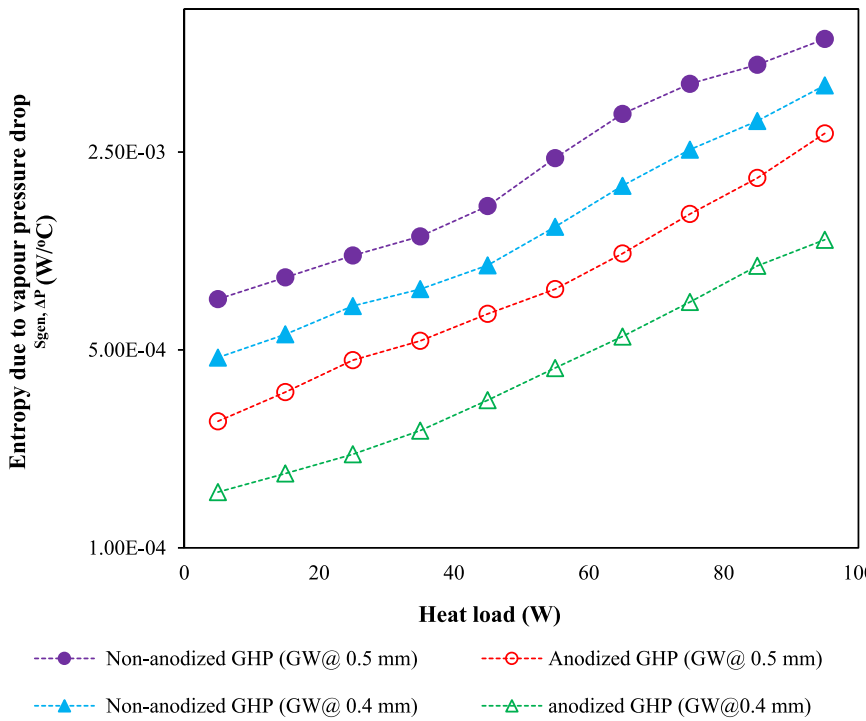

FIGURE 4 Impact of anodization on entropy due to vapor pressure drop of GHP. GHP, grooved heat pipe; GW, groove width.

26884542, 2025, 1, Downloaded from https://onlinelibrary.wiley.com/doi/10.1002/htj.23193 by University Of Pretoria, Wiley Online Library on [06/08/2025]. See the Terms and Conditions (https://onlinelibrary.wiley.com/terms-and-conditions) on Wiley Online Library for rules of use; OA articles are governed by the applicable Creative Commons License

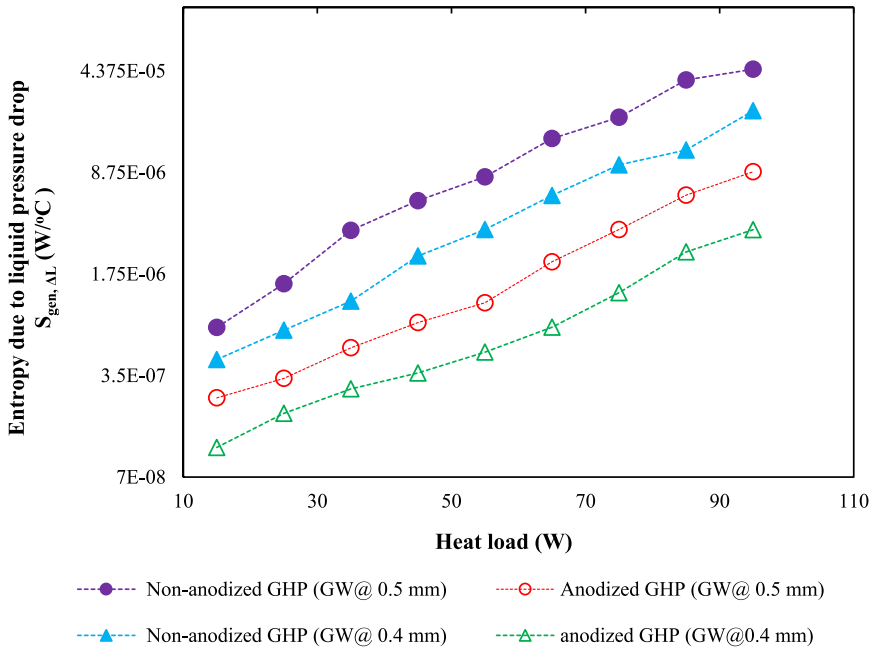

FIGURE 5 Impact of anodization on entropy due to liquid pressure drop in GHP. GHP, grooved heat pipe; GW, groove width.

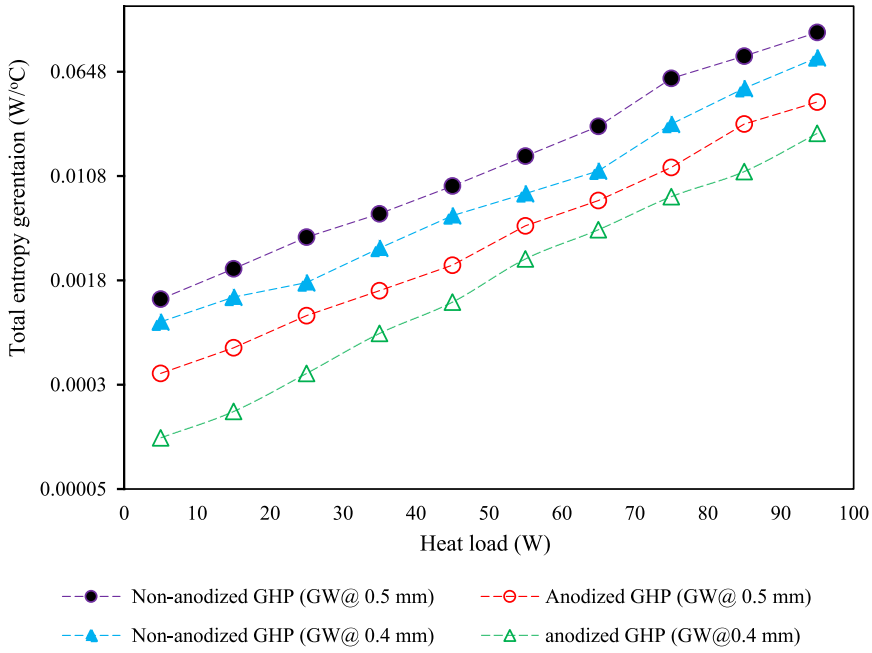

FIGURE 6 Impact of anodic oxidization on the total entropy production of GHP. GHP, grooved heat pipe; GW, groove width.

26884542, 2025, 1, Downloaded from https://onlinelibrary.wiley.com/doi/10.1002/htj.23193 by University Of Pretoria, Wiley Online Library on [06/08/2025]. See the Terms and Conditions (https://onlinelibrary.wiley.com/terms-and-conditions) on Wiley Online Library for rules of use; OA articles are governed by the applicable Creative Commons License

4.3 | Impact of anodization on the total entropy generation of GHP

The sum of the entropy due to heat transfer and the pressure drop brought on by the movement of liquid and vapor constitutes the total entropy generation. The total entropy generation of GHP at an optimum inclination angle of 45° is found using Equation (12) and illustrated in Figure 6. Theoretically, it is assumed that the system (GHP) is adiabatic (constant temperature) as there is nil heat loss. However, for the experimentation, there will be some heat loss (change in temperature drop), which indicates the system will not be fully adiabatic. Figure 6 shows a linear increase in total entropy generation with an increase in heat load. Moreover, comparing all four cases, a total entropy reduction of about 0.022 W/°C is attained at the maximum heat input of 95 W for anodized GHP with a GW of 0.4 mm.

4.4 | Impact of anodization on the Bejan number of GHP

The effect of anodization on the Bejan number for the two sets of GHP at an optimum tilt angle of 45° with increased heat load is estimated using Equation (13) and presented in Figure 7. Bejan number denotes the proportion of irreversibility or the ratio of entropy generation due to heat transfer to the total irreversibility. Bejan number values range from 0 to 1. Therefore, if $Be > 0.5$, irreversibility in heat transfer dominates the frictional fluid flow, and if $Be < 0.5$, frictional entropy dominates the heat transfer irreversibility. Experimental results show $Be < 0.5$ at initial heat loads, which indicates the frictional entropy dominates the heat transfer irreversibility, whereas, for all the remaining conditions, Be shows a value >0.5, which indicates heat transfer irreversibility got dominated. From Figure 7, it was observed that the Bejan number rises with an

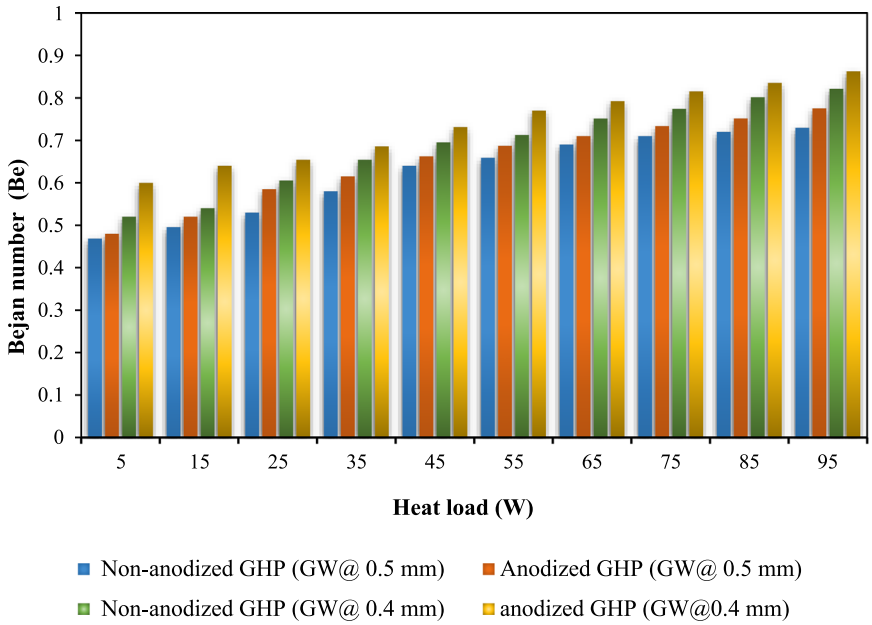

FIGURE 7 Impact of anodization on the Bejan number for the two sets of GHP. GHP, grooved heat pipe; GW, groove width.

26884542, 2025, 1, Downloaded from https://onlinelibrary.wiley.com/doi/10.1002/htj.23193 by University Of Pretoria, Wiley Online Library on [06/08/2025]. See the Terms and Conditions (https://onlinelibrary.wiley.com/terms-and-conditions) on Wiley Online Library for rules of use; OA articles are governed by the applicable Creative Commons License

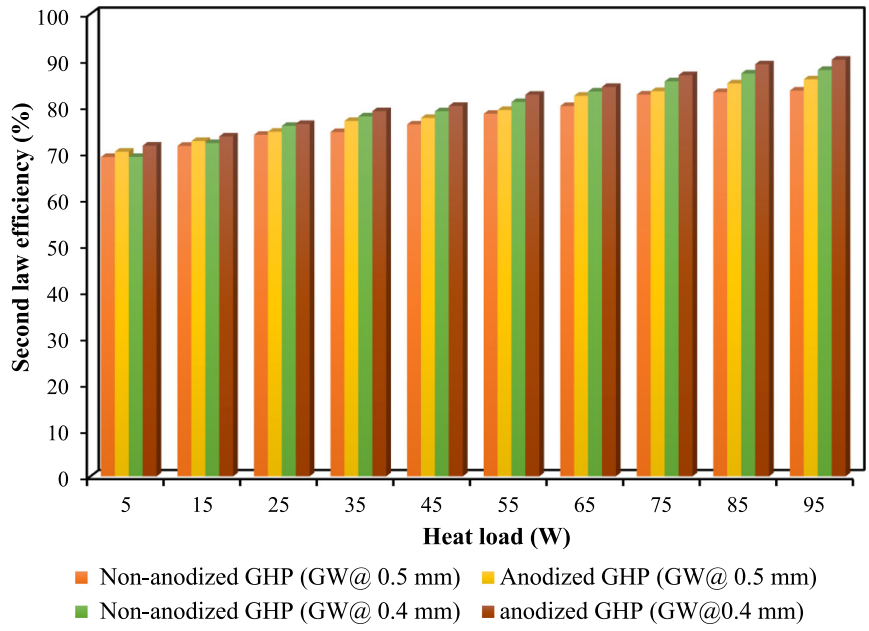

FIGURE 8 Impact of anodic oxidization on the second-law efficiency of GHP. GHP, grooved heat pipe; GW, groove width.

increase in heat load. Furthermore, at the initial heat load for nonanodized and anodized GHP having a GW of 0.5 mm, the Bejan number falls below 0.5, illustrating that the irreversibility due to frictional fluid flow dominates the irreversibility due to temperature difference. However, for increased heat loads, the Bejan number rises above 0.5, suggesting that the GHP's heat transfer influences the irreversibility due to frictional fluid flow.

4.5 | Impact of anodic oxidization on the second-law efficiency of GHP

The impact of anodic oxidization on the second-law efficiency for the GHPs with a rise in heat load is estimated by Equation (14) and shown in Figure 8. The second-law efficiency is used to assess the effectiveness of the GHPs associated with their reversible heat transfer performance. Figure 8 shows that the second-law efficiency for the two sets of GHPs increases linearly with a rise in heat load. Further, at an optimum inclination angle of 45°, a highest efficiency of 89.12% is found for anodized GHP with a GW of 0.4 mm and a minimum efficiency of 69.13% for nonanodized GHP with a GW of 0.5 mm.

5 | CONCLUSIONS

The entropy analysis of an anodic oxidized GHP having a groove width of 0.5 and 0.4 mm at an optimum inclination of 45° charged with anhydrous ammonia was studied and presented. This study includes the impact of anodization on entropy generation due to heat transfer, vapor

26884542, 2025, 1, Downloaded from https://onlinelibrary.wiley.com/doi/10.1002/htj.23193 by University Of Pretoria, Wiley Online Library on [06/08/2025]. See the Terms and Conditions (https://onlinelibrary.wiley.com/terms-and-conditions) on Wiley Online Library for rules of use; OA articles are governed by the applicable Creative Commons License

flow, liquid flow, total entropy generation, Bejan number, and second-law efficiency for the two sets of GHPs. The following conclusions arrived based on the above analysis:

- A minimum entropy generation due to heat transfer of 0.015 W/°C and a minimum entropy generation due to pressure drop in a vapor of 0.00125 W/°C is obtained for anodized GHP having a groove width of 0.4 mm. For the same GHP, the liquid pressure drop of 3.5e − 6 W/°C is obtained.
- A total entropy generation of 0.0385 W/C is obtained for an anodized GHP having a groove width of 0.4 mm.
- Similarly, a maximum second-law efficiency of 89.12% is obtained with an anodized GHP having a groove width of 0.4 mm.

Results affirmed that the decrease in groove width along thin porous coating through anodization in the GHP was the prime reason for the entropy reduction.

NOMENCLATURE

$C_{p,l}$	specific heat capacity of liquid (J/kg K)
GHP	grooved heat pipe
GW	groove width (mm)
HP	heat pipe
K	permeability
L_t	total length (m)
MWCNT	multiwalled carbon nanotubes
PDE	partial differential equation
Δp	drop in pressure (Pa)
R_v	vapor channel radius (m)
S	entropy (J/(kg K))
T	temperature (C)

GREEK SYMBOLS

Δ	delta
η	efficiency
μ_v	vapor viscosity (N s/m^2)
ρ_v	vapor density (kg/m^3)
θ	inclination angle

SUBSCRIPTS

a	adiabatic
c, w	condenser wall
eff	effective
e, w	evaporator wall
HT	heat transfer
l	liquid
t	total length
v	vapor

26884542, 2025, 1, Downloaded from https://onlinelibrary.wiley.com/doi/10.1002/htj.23193 by University Of Pretoria, Wiley Online Library on [06/08/2025]. See the Terms and Conditions (https://onlinelibrary.wiley.com/terms-and-conditions) on Wiley Online Library for rules of use; OA articles are governed by the applicable Creative Commons License

ACKNOWLEDGMENTS

The authors would like to acknowledge DST–SERB for the financial support they received to conduct this research under the sanction order DST/SERB/YSS/2015/001084.

DATA AVAILABILITY STATEMENT

The data that support the findings of this study are available on request from the corresponding author. The data are not publicly available due to privacy or ethical restrictions.

ORCID

Madhu Ganesh http://orcid.org/0000-0002-2999-2547
Mohsen Sharifpur http://orcid.org/0000-0003-1302-1954

REFERENCES

1. Dorf RC. *The Electronic Handbook*. IEEE Press; 1996.
2. Ghanbarpour M, Khodabandeh R. Entropy generation analysis of cylindrical heat pipe using nanofluid. *Thermochim Acta*. 2015;610:37-46. doi:10.1016/j.tca.2015.04.028
3. Xie K, Ji Y, Yu C, Wu M, Yi H. Experimental investigation on an aluminum oscillating heat pipe charged with water. *Appl Therm Eng*. 2019;162:114182. doi:10.1016/j.applthermaleng.2019.114182
4. Cui X, Qiu Z, Weng J, Li Z. Heat transfer performance of closed loop pulsating heat pipes with methanol-based binary mixtures. *Exp Therm Fluid Sci*. 2016;76:253-263. doi:10.1016/j.expthermflusci.2016.04.005
5. Hao T, Ma H, Ma X. Heat transfer performance of polytetrafluoroethylene oscillating heat pipe with water, ethanol, and acetone as working fluids. *Int J Heat Mass Transfer*. 2019;131:109-120. doi:10.1016/j.ijheatmasstransfer.2018.08.133
6. Wang PY, Chen XJ, Liu ZH, Liu YP. Application of nanofluid in an inclined mesh wicked heat pipes. *Thermochim Acta*. 2012;539:100-108. doi:10.1016/j.tca.2012.04.011
7. Karthikeyan VK, Ramachandran K, Pillai BC, Brusly Solomon A. Effect of nanofluids on thermal performance of closed loop pulsating heat pipe. *Exp Therm Fluid Sci*. 2014;54:171-178. doi:10.1016/j.expthermflusci.2014.02.007
8. Alizad K, Vafai K, Shafahi M. Thermal performance and operational attributes of the startup characteristics of flat-shaped heat pipes using nanofluids. *Int J Heat Mass Transfer*. 2012;55(1-3):140-155. doi:10.1016/j.ijheatmasstransfer.2011.08.050
9. Sun Y, Liang F, Tang H, Tang Y, Zhang S, Chua KJ. Ultrathin flexible heat pipes with *Microsorum fortunei* structural-like wick for cooling flexible electronic devices. *Int J Heat Mass Transfer*. 2023;202:123743. doi:10.1016/j.ijheatmasstransfer.2022.123743
10. Tang H, Tang Y, Wu X, Peng R, Sun Y. Fabrication and capillary characterization of multi-scale micro-groove wicks for ultrathin phase-change heat transfer devices. *Appl Therm Eng*. 2023;219(PB):119621. doi:10.1016/j.applthermaleng.2022.119621
11. Heng Tang YS, You J, Tang Y, Guo B. Pool boiling heat transfer performance of micro-embossing molds for the fabrication of polymer wicks. *Phys Fluids*. 2024:023346.
12. Vasiliev LL, Grakovich LP, Rabetskii MI, et al. Grooved heat pipes with a nanoporous deposit in an evaporator. *Heat Pipe Sci Technol Int J*. 2010;1(3):219-236. doi:10.1615/heatpipescietech.2011002703
13. Solomon ABB, Roshan R, Vincent W, Karthikeyan VKK, Asirvatham LGG. Heat transfer performance of an anodized two-phase closed thermosyphon with refrigerant as working fluid. *Int J Heat Mass Transfer*. 2015;82:521-529. doi:10.1016/j.ijheatmasstransfer.2014.11.034
14. Solomon ABB, Ram Kumar AM, Ramachandran K, et al. Characterisation of a grooved heat pipe with an anodised surface. *Heat Mass Transfund Stoffuebertragung*. 2017;53(3):753-763. doi:10.1007/s00231-016-1856-8
15. Sudhan ALS, Solomon AB, Sunder S. Heat transport limitations and performance enhancement of anodized grooved heat pipes charged with ammonia under gravity and anti-gravity condition. *Appl Therm Eng*. 2022;200:117633. doi:10.1016/j.applthermaleng.2021.117633
16. Khalkhali H, Faghri A, Zuo ZJ. Entropy generation in a heat pipe system. *Appl Therm Eng*. 1999;19(10):1027-1043. doi:10.1016/S1359-4311(98)00089-1

26884542, 2025, 1, Downloaded from https://onlinelibrary.wiley.com/doi/10.1002/htj.23193 by University Of Pretoria, Wiley Online Library on [06/08/2025]. See the Terms and Conditions (https://onlinelibrary.wiley.com/terms-and-conditions) on Wiley Online Library for rules of use; OA articles are governed by the applicable Creative Commons License

17. Kim S, Zhang Y, Choi J. Entropy generation analysis for a pulsating heat pipe. *Heat Transfer Res*. 2013;44(1):1-30. doi:10.1615/HeatTransRes.2012005734
18. Akbarzadeh M, Rashidi S, Keshmiri A. The optimum position of porous insert for a double-pipe heat exchanger based on entropy generation and thermal analysis. *J Therm Anal Calorim*. 2019;139:411-426. doi:10.1007/s10973-019-08362-x
19. Jafarmadar S, Azizinia N, Razmara N, Mobadersani F. Thermal analysis and entropy generation of pulsating heat pipes using nanofluids. *Appl Therm Eng*. 2016;103:356-364. doi:10.1016/j.applthermaleng.2016.03.032
20. Kumar S, Manoj S, Moharana K. Thermo-hydraulic and entropy generation analysis of recharging microchannel using water-based graphene–silver hybrid nanofluid. *J Therm Anal Calorim*. 2021;143:4131-4148. doi:10.1007/s10973-020-09382-8
21. Chopra K, Tyagi VV, Pandey AK. Thermodynamic and techno-economic analysis of heat pipe ETC water heating system for Indian composite climate an experimental approach. *J Therm Anal Calorim*. 2020;139:1395-1407. doi:10.1007/s10973-019-08487-z
22. Khosravi-Bizhaem H, Abbassi A, Salimpour MR, Zivari-Ravan A. Experimental study on heat transfer, entropy generation, and exergy destruction of Ag, MWCNT, and GO water-based nanofluids in helical tubes. *J Therm Anal Calorim*. 2022;147(3):2761-2784. doi:10.1007/s10973-021-10655-z
23. Maqbool SSK, Sadiq RE. Heat transfer analysis of tangent hyperbolic nanofluid in a ciliated tube with entropy generation. *J Therm Anal Calorim*. 2021;144:2337-2346. doi:10.1007/s10973-021-10681-x
24. Ersöz MA, Yildiz A. Thermoeconomic analysis of thermosyphon heat pipes. *Renew Sustain Energy Rev*. 2016;58:666-673. doi:10.1016/j.rser.2015.12.250
25. Hari R, Muraleedharan C. Analysis of effect of heat pipe parameters in minimising the entropy generation rate. *J Thermodyn*. 2016;2016. doi:10.1155/2016/1562145
26. Behrooz HS, Ziapour M. Exergetic analysis of a long two-phase closed thermosyphon system. *Int J Exergy*. 2021;7:714-730. doi:10.1504/IJEX.2010.035517
27. Sriram Sudhan AL, Brusly Solomon A. *Effect of Temperature on the Surface Characteristics of Anodized Aluminium Tubes*. Springer Singapore; 2021. doi:10.1007/978-981-15-4745-4_52

How to cite this article: Brusly Solomon A, Jims John Wessley G, Ganesh M, Sharifpur M, Rethinam RS. Influence of anodizati Phys Fluids.on on the entropy generation in grooved heat pipes. *Heat Transfer*. 2025;54:609-625. doi:10.1002/htj.23193

26884542, 2025, 1, Downloaded from https://onlinelibrary.wiley.com/doi/10.1002/htj.23193 by University Of Pretoria, Wiley Online Library on [06/08/2025]. See the Terms and Conditions (https://onlinelibrary.wiley.com/terms-and-conditions) on Wiley Online Library for rules of use; OA articles are governed by the applicable Creative Commons License